Designing sustainable high-strength self-compacting concrete with high content of supplementary cementitious materials

Abdullah Alshahrani [a,b], Tianyi Cui [a], Ayman Almutlaqah [a,b], Sivakumar Kulasegaram [a, *]

[a] School of Engineering, Cardiff University, Cardiff, UK
[b] Civil Engineering Department, College of Engineering, Najran University, Najran, Saudi Arabia
[*] Corresponding author. E-mail address: kulasegarams@cardiff.ac.uk

Abstract

A sustainable and green approach to concrete mix design is fundamental for the construction sector in terms of reducing carbon dioxide (CO_2) emissions and conserving non-renewable natural resources. This paper proposes a novel mix design method for sustainable high-strength self-compacting concrete (HSSCC) based on rheological and mechanical properties with the aim of reducing cement content in such mixes. HSSCC mixes were designed using ground granulated blast furnace slag (GGBS) and fly ash to replace up to 40% of the cement content and tested for target compressive strengths ranging between 70 and 100 MPa. The proposed design method was numerically programmed to provide straightforward and realistic guidance in the form of design charts, and verified through the design and production of sixteen HSSCC mixes consisting of varying sand-to-aggregate ratios (S/A). All mixes satisfied the self-compacting concrete criteria in the fresh state and achieved the targeted viscosity and compressive strength values. The effects of S/A and paste-to-solid (P/S) ratios on the rheological properties were evaluated. The experimental results demonstrated that the proposed mix design method could produce HSSCC with excellent fresh and mechanical characteristics while being eco-efficient with respect to CO_2 emissions and cement consumption.

Keywords: Self-compacting concrete; high performance; supplementary cementitious materials; fresh tests; compressive strength

Word count: 5474

1. Introduction

Concrete is the most widely used construction material, with a global consumption of approximately 30 billion tonnes every year (Thomas et al., 2021). This large concrete usage can be attributed to its multiple advantages, such as worldwide availability of raw materials, low-cost production, and durability in harsh environments. However, the global carbon dioxide (CO_2) emissions emitted during the production and transportation of concrete form approximately 10% of the total anthropogenic CO_2 in the environment (Long et al., 2015). The carbon footprint of concrete is predominantly caused by the production of ordinary Portland cement (OPC), accounting for approximately 5% to 7% of the annual CO_2 emissions (Berndt, 2015; Celik et al., 2015; de Grazia et al., 2019). Furthermore, the construction industry consumes a significant quantity of non-renewable resources during the concrete manufacturing process, such as natural river sand (Sivakrishna et al., 2020). The predicted future increase in concrete production is expected to result in considerable depletion of natural resources and pollution of the environment (Gupta et al., 2021). Therefore, to meet the predicted concrete demands, it is essential to develop sustainable and eco-friendly concrete production processes to reduce CO_2 emissions and conserve non-renewable natural resources.

Self-compacting concrete (SCC) can be considered as one of the greatest innovations in concrete technology; its production has increased rapidly due to its superior material properties and multiple applications. When placed in formwork, SCC can pass through areas of congested reinforcement under its own weight and without the need for external vibration (Okamura & Ouchi, 1999). Compared to conventional concrete, SCC has a reduced construction time and enhanced quality and durability. However, it often requires a greater quantity of cement than conventional concrete. This high cement demand can increase the cost of SCC and pose a sustainability threat to the environment (Adesina & Awoyera, 2019). The production of one tonne of OPC emits approximately one tonne of carbon dioxide emissions (Kaish et al., 2018); therefore, significant research has been devoted to the development of eco-friendly and sustainable self-compacting concrete.

The concept of sustainable SCC production encompasses the eco-friendly utilisation of industrial by-products while providing a feasible alternative for the raw construction materials used in concrete production. The utilisation of alternative materials as a replacement for traditional SCC constituents will not only make SCC more sustainable but will impart many advantages, such as cost reduction, eco-consumption of by-products, natural resource conservation, environmental protection from pollutants, and landfill cost-saving (Gupta et al., 2021). Several industrial waste materials, such as limestone powder, fly ash, slag, sawdust ash, silica fume, and rice husk ash, have been used in the production of SCC in the past. However, most industrial waste materials are either disposed of or used without fully exploiting their beneficial characteristics. (Jalal et al., 2015). Further research is required to develop a sustainable SCC using waste materials, with a particular focus on optimal mix designs (Adesina & Awoyera, 2019). In addition, it is important to evaluate the rheological properties and the long-term effect of these materials on the hardened properties of SCC. Among these industrial waste materials, ground granulated blast furnace slag (GGBS) and fly ash have been reported as being able to alter and enhance the fresh and mechanical properties of concrete, as well as the durability thereof (Adesina & Awoyera, 2019; Jalal et al., 2015; Nehdi et al., 2004). Despite these findings, only a small fraction of the fly ash and GGBS produced globally is harnessed in the construction industry. For example, Turkey generates 13 million tonnes of fly ash annually, yet it utilises only 5% of this waste product in construction (Jalal et al., 2015). Moreover, 90 million tonnes of GGBS are utilised in manufacturing concrete annually, while the production of GGBS is approximately 250 tonnes per year (Al-Oran et al., 2019). Therefore, exploiting the potential of GGBS and fly ash in the production of SCC will enhance the sustainability performance of SCC.

A suggested approach for the construction industry to decrease its CO_2 footprint is to reduce the amount of concrete used in structures through the use of high-strength concrete (HSC), which performs similar to conventional concrete but uses substantially less concrete for the same strength (Campos et al., 2020; de Matos et al., 2019). In addition to the overall reduction of concrete volumes, using HSC often results in improved durability and lower raw material consumption. Aïtcin (2019) suggested that increasing the compressive strength of concrete would reduce the quantity of concrete required to support the loads exerted on a structure, thereby reducing cement usage. Concrete efficiency can be defined as the total amount of cement required in a concrete mix to produce one unit of compressive strength (Campos et al., 2020). As the compressive strength increases, the cement consumption per cubic meter of concrete (kg/m^3) reduces per unit of compressive strength (MPa) (Campos et al., 2020; Yousuf et al., 2019). In conventional concrete, the ratio between the volume of the cement and its compressive strength typically varies from 9 to 14 $(kg/m^3)/MPa$ (de Grazia et al., 2019). In contrast, the ratios for HSC are in the region of 5 $(kg/m^3)/MPa$ (Damineli et al., 2010), indicating greater concrete efficiency. Furthermore, as the compressive strength of the concrete increases, the CO_2 release per MPa correspondingly decreases (Campos et al., 2019). Campos et al. (2020) concluded that HSC is not only preferable in terms of the environment but also economically advantageous due to the reduction of cement consumption.

This study aimed to develop a sustainable version of HSSCC by optimising the replacement level of supplementary cementitious materials while maintaining or exceeding the fresh and mechanical properties of an unmodified concrete mix. A new design method for sustainable HSSCC mixes is proposed based on rheological characteristics and mechanical properties, wherein carbon dioxide emissions and cement consumption can be reduced compared to the standard mix proportioning of HSSCC. For experimental validation of this method, 16 mixes of HSSCC with different compositions were designed, produced, and evaluated in fresh and hardened states. The sustainability of the test mixes was estimated and compared to that reported in the literature for HSSCC and HSC conventional mixes.

2. Proposed mix design method for sustainable HSSCC

Although research on SCC has been ongoing since the early 1970s, the invention of SCC was attributed to Okamura in 1988 (Okamura & Ozawa, 1996). Since then, various mix design methods have been developed based on different principles and parameters, such as empirical, statistical factorial, aggregate packing, compressive strength, and paste rheology methods (Shi et al., 2015). Karihaloo, Ghanbari, and Deeb (Deeb et al., 2012; Deeb & Karihaloo, 2013; Karihaloo & Ghanbari, 2012) suggested a mix design approach based on plastic viscosity for proportioning conventional and HSSCC mixes, although the compressive strength was not explicitly considered as a design parameter. This method takes advantage of the plastic viscosity expression for SCC mixes and proposes a mix design procedure accordingly. This design approach could potentially limit laboratory work and the utilisation of resources while providing a foundation for quality management. Abo Dhaheer et al. (2016b) subsequently introduced compressive strength as a design parameter of SCC. They developed a basic mix proportioning approach for compressive strengths up to 80 MPa.

The current study proposes a mix-proportioning method for HSSCC combining these two approaches based on the target compressive strength and plastic viscosity, with increased supplementary cementitious material (SCM) content. This methodology is suitable for a wide range of HSSCC compressive strengths (70 MPa to 100 MPa) and offers practical guidelines to corroborate the effectiveness and simplicity of this approach.

2.1. Compressive strength target

It is well-recognised that the compressive strength of SCC is mainly determined by the ratio of water to cementitious materials (w/cm), as well as the composition of the cementitious materials used (Domone, 2006). However, the compressive strength of SCC is dominantly affected by the w/cm rather than the total paste volume (Jawahar et al., 2013). Several empirical equations have been proposed for calculating compressive strength from w/cm based on the well-known Abrams rule (Abo Dhaheer et al., 2016a; Aggarwal & Aggarwal, 2019). Abo Dhaheer et al. (2016a) adopted the following equation to calculate the 28-day compressive strength (f_{cu}) of cubes cast from SCC mixes:

$$f_{cu} = \frac{195}{12.65^{w/cm}} \tag{1}$$

This equation was validated through extensive testing for SCC mixes with compressive strengths between 30 and 80 MPa. From the results, it was recommended that the w/cm should be reduced by 14% and 8% for 30 MPa and 40 MPa mixes, respectively. This equation is adopted and validated in the present study for mixes with compressive strengths up to 100 MPa.

2.2. Plastic viscosity target

The plastic viscosity of a homogeneous viscous fluid, such as cement paste made up of cement, water, SCMs, and superplasticiser (SP), can be measured using a conventional viscometer with a reasonable degree of accuracy. However, this is not possible for a non-homogeneous viscous fluid such as a self-compacting concrete mix. Many researchers have established that samples drawn from one SCC mix show different plastic viscosities when measured with different rheometers (Feys et al., 2007; Feys &

Khayat, 2013; Wallevik & Wallevik, 2011). Therefore, to overcome these inconsistent viscosity values, Karihaloo and Ghanbari proposed a micro-mechanical model to estimate the plastic viscosity of SCC mixes based on the plastic viscosity of the paste (Ghanbari & Karihaloo, 2009). Although their research compared SCC mixes both with and without fibres, other researchers have adopted this concept to predict the plastic viscosity of standard SCC mixes without fibres (Abo Dhaheer et al., 2016a, 2016b; de la Rosa et al., 2018; Deeb et al., 2012; Deeb & Karihaloo, 2013).

For this approach to be utilised, it is necessary to first establish the plastic viscosity of the homogeneous paste. The micro-mechanical procedure treats the SCC mix as a two-phase suspension, where the solid phase, consisting of aggregates and other solids, is suspended in the liquid phase (cement paste). The suspension model estimates the increase in plastic viscosity of the liquid phase as a result of the addition of the solid phase. Initially, the finest solid, i.e., the sand, is considered as being in the viscous liquid phase. The coarse aggregate is designated as the solid phase and is suspended in the viscous fluid phase from step one. The process is repeated until all the solid constituents have been incorporated.

The plastic viscosity of an i^{th} liquid-solid suspension can be estimated from the plastic viscosity of the preceding $(1 - i)^{th}$ phase using Equation 2:

$$\eta_i = \eta_{i-1} * f_i(\phi_i) \tag{2}$$

where

η_i plastic viscosity of the i^{th} liquid-solid suspension

η_{i-1} plastic viscosity of the preceding $(1 - i)^{th}$ phase

$f_i(\phi_i)$ factor greater than one, which predicts the increase in the plastic viscosity attributed to a solid phase having a volume fraction of ϕ_i

For the initial step, $i = 1$, implying η_0 is the plastic viscosity of the paste. The plastic viscosity of SCC can thus be estimated as shown in Equation 3:

$$\eta_{mix} = \eta_{paste} * f_1(\phi_1) * f_2(\phi_2) * f_3(\phi_3) * \cdots * f_n(\phi_n) \tag{3}$$

where

n total number of solid phases in the mixture.

In addition to the fine and coarse aggregate, air voids are considered as a second phase in a viscous suspension. Einstein was the first to derive a basic equation for the viscosity of a dilute suspension (defined as a suspension having a second phase volume fraction less than 10%) of hollow or rigid spheres with no hydrodynamic interactions (Struble & Sun, 1995). He developed an expression $f_i(\phi_i)$ for suspensions with simple shapes such as spheres and spheroids in Newtonian fluids, where the expression $f_i(\phi_i)$ depended solely on the solid volume fraction ϕ_i and should be less than 10% (Koehler & Fowler, 2007). Einstein's approximation for $f_i(\phi_i)$ is indicated in Equation 4:

$$f_i(\phi_i) = 1 + [\eta]\phi_i \tag{4}$$

where

η intrinsic viscosity of the suspension

The numerical factor η for air bubbles in suspension and rigid spherical particles with random hexagonal packing arrangements is 2.5 and 1, respectively. Further studies have determined that a numerical factor of 2.5 is suitable for rigid ellipsoidal particles with aspect ratios less than 3 (Koehler & Fowler, 2007; Struble & Sun, 1995). At higher volume fractions, hydrodynamic interactions and the random motion of suspended particles became significant. In such cases, the Krieger-Dougherty formula can be used to calculate $f_i(\phi_i)$ (Krieger & Dougherty, 1959) as indicated in Equation 5; this approach was considered appropriate for calculating viscosity in concentrated cementitious suspensions.

$$f_i(\phi_i) = \left(1 - \frac{\phi_i}{\phi_m}\right)^{-[\eta]\phi_m} \tag{5}$$

where

ϕ_i volume fraction of the dispersed solid phase of the suspension

ϕ_m maximum packing fraction of particles in the dispersed solid phase

η dynamic viscosity of the suspension

The Krieger-Dougherty formula shows the dependence of $f_i(\phi_i)$ on the maximum packaging fraction and the dynamic viscosity of the suspension. The maximum packing fraction, ϕ_m, is a measure of the concentration of solid particles that can be added to a viscous phase while maintaining flowability. The dynamic viscosity of the suspension, η, indicates the effect of individual particles on the viscosity. Both ϕ_m and η are affected by the rate of shear applied to the system. The maximum packaging fraction, ϕ_m, has a proportional relationship with the shear rate, whereas the dynamic viscosity, η, is inversely proportional and decreases with increasing shear rate. Thus, the final product of ϕ_m and η remains approximately equal to 1.9 for rigid spherical particles (de Kruif et al., 1985).

The proportion of fine and coarse aggregates in HSSCC mixes exceeds 10%. Hence, their effect on the known plastic viscosity of paste can be determined from the Krieger-Dougherty equation in Equation 5. Trapped air bubbles account for approximately 2% of the volume fraction at high volume fractions. Thus, Einstein's approximation for $f_i(\phi_i)$ (refer to Equation 4) with the numerical factor equal to 1 can be used to account for trapped air bubbles. Substituting Equations 4 and 5 into Equation 3, and assuming a 2% increase in plastic viscosity due to trapped air, the plastic viscosity of the mix can be calculated from Equation 6.

$$\eta_{mix} = \eta_{paste} * \left(1 - \frac{\phi_{\text{fine agg}}}{\phi_m}\right)^{-1.9} * \left(1 - \frac{\phi_{\text{coarse agg}}}{\phi_m}\right)^{-1.9} \quad (6)$$

where

$\phi_{\text{fine agg}}$ volume fraction of the fine aggregate in the suspension

$\phi_{\text{coarse agg}}$ volume fractions of the coarse aggregate in the suspension

The packing density (maximum packing fraction, ϕ_m) increases with the addition of the solid phases. As suggested by Abo Dhaheer et al. (2016a), adding fine aggregate to the paste can be considered as random hexagonal packing with ϕ_m equal to 0.63. When the last solid phase (coarse aggregate) is added to the suspension, the packing becomes dense and can be considered as close hexagonal packing with ϕ_m equal to 0.74 (Abo Dhaheer et al., 2016a).

2.3. Method steps

The proposed design mix methodology for HSSCC was programmed in MATLAB to provide design charts, as illustrated in Figure 1, with the procedural steps outlined in Figure 2. Table 1 shows the mass and volume ranges of typical SCC compositions according to the European Guidelines for Self-

Compacting Concrete (EFNARC) (2005), which can be used to determine water content and mix proportions. Four HSSCC mixes were designed for different compressive strengths (70, 80, 90, and 100 MPa) based on plastic viscosity. The plastic viscosity of the pastes was obtained from viscometer tests; the test results are indicated in Table 2. An example of mix proportioning and calculations is presented in the Appendix.

Table 1. Typical range of SCC mix compositions according to EFNARC (2005)

Constituent	Typical range by mass (kg/m^3)	Typical range by volume ($litres/m^3$)
Cementitious material	380–600	−−
Paste	−−	300–380
Water	150–210	150–210
Coarse aggregate	750–1000	270–360
Fine aggregate	48–55% of total agg. weight	
Water/cm ratio by Vol.	0.85–1.10	

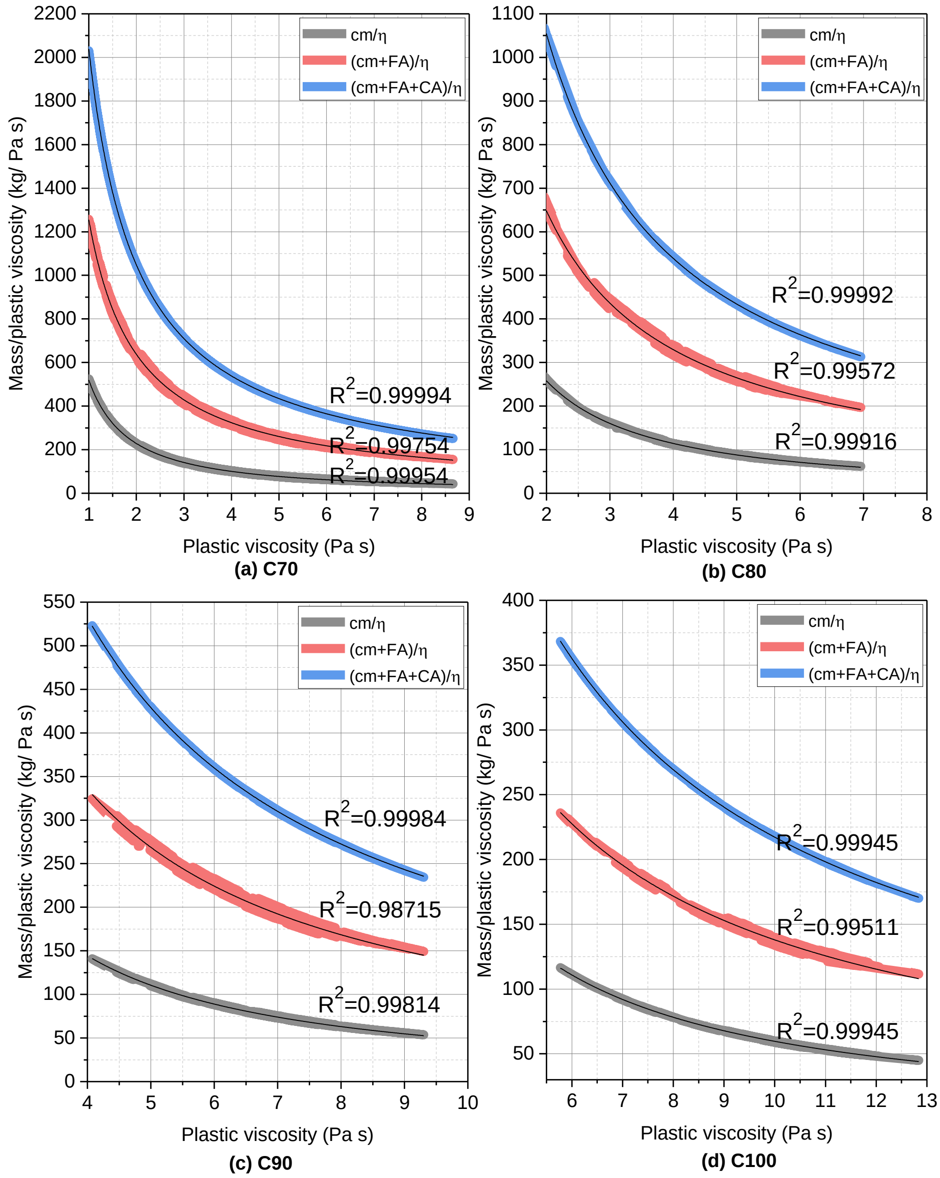

Figure 1. Design charts of concrete grades based on plastic viscosity a) C70, b) C80, c) C90, and d) C100

Table 2. Plastic viscosity of the paste (60% CEM I, 20% GGBS, 20% fly ash, SP, and water)

Mix code	w/cm	η_{paste} (Pa·s)	$\eta_{paste+air}$ (Pa·s)
C70	0.40	0.053	0.054
C80	0.35	0.073	0.075
C90	0.30	0.177	0.18
C100	0.26	0.381	0.39

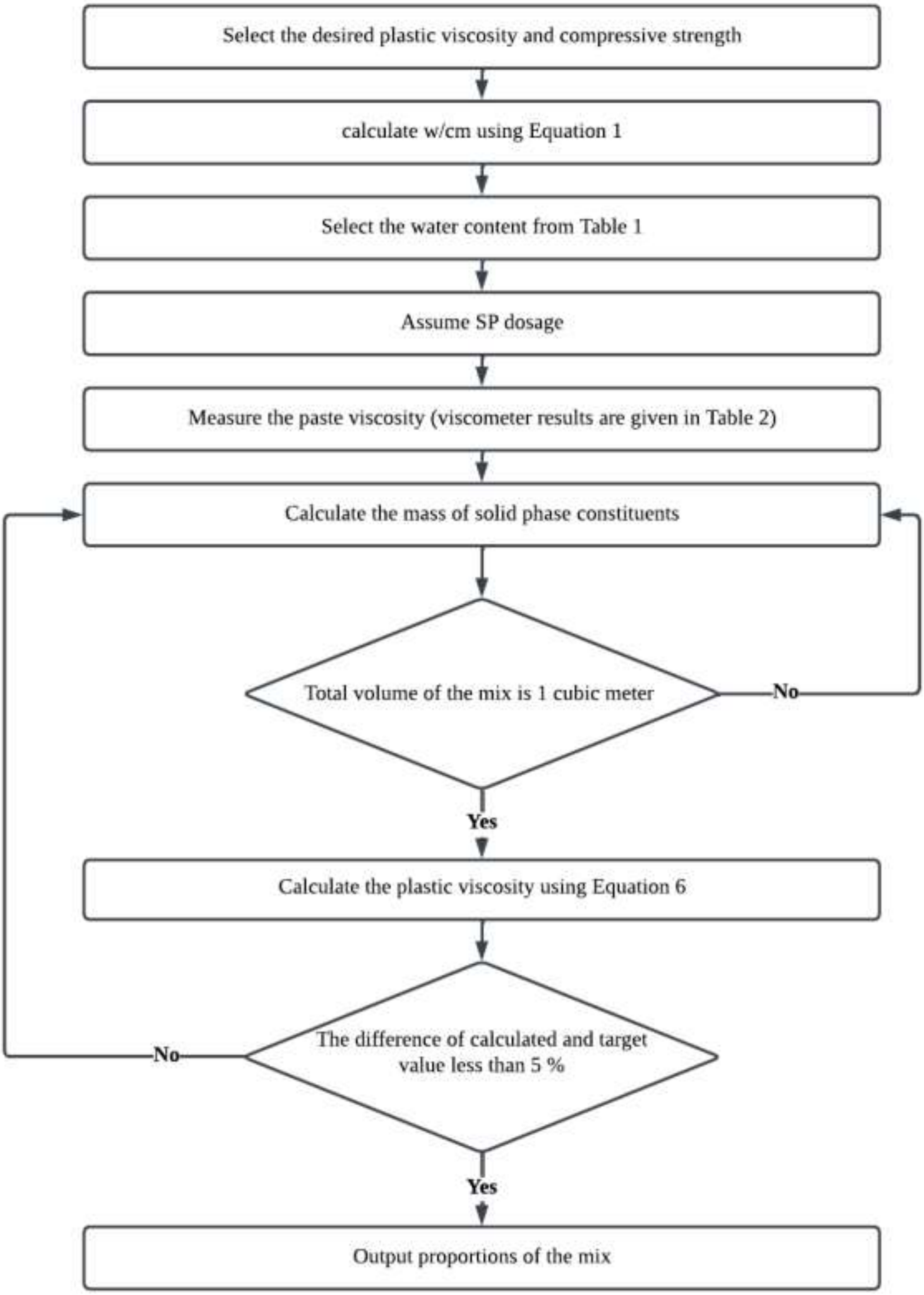

Figure 2. The procedure of the proposed methodology of HSSCC mix proportions

3. Experimental method validation

3.1. Materials

The materials used in the experimental mixes comprised OPC, GGBS, fly ash, and superplasticiser (SP). The OPC had a compressive strength grade of 52.5 MPa, a specific gravity of 3.15, and a fineness of 384 m^2/kg. GGBS and fly ash were added as cementitious materials, each with a specific gravity of 2.4, while the SP was MasterGlenium ACE 499, a polycarboxylate ether polymer with a specific gravity of 1.07. The chemical composition of the cementitious materials is indicated in Table 3.

Table 3. The chemical composition of the cementitious binder materials

Composition	SiO_2	Al_2O_3	Fe_2O_3	CaO	K_2O	Na_2O	MgO	So_3	TiO_2
OPC	19.69	4.32	2.85	63.04	0.74	0.16	2.17	3.12	0.33
GGBS	34.34	12.25	0.32	39.90	0.45	0.41	7.70	0.23	0.65
Fly ash	53.10	20.64	8.93	6.12	2.17	1.68	1.79	1.93	0.90

The aggregates consisted of crushed limestone coarse aggregate (CA) with a specific gravity of 2.65 and a maximum stone size of 20 mm, and natural river sand as fine aggregate (FA) with a specific gravity of 2.55 and a maximum particle size of 2 mm. Approximately 30% of the fine aggregate was replaced with a coarser fraction of limestone dust (LD) (crushed rock sand) with a specific gravity of 2.6 and particle size ranging between 0.125 mm and 2 mm. The particle size distribution curves of fine and coarse aggregates are shown in Figure 3.

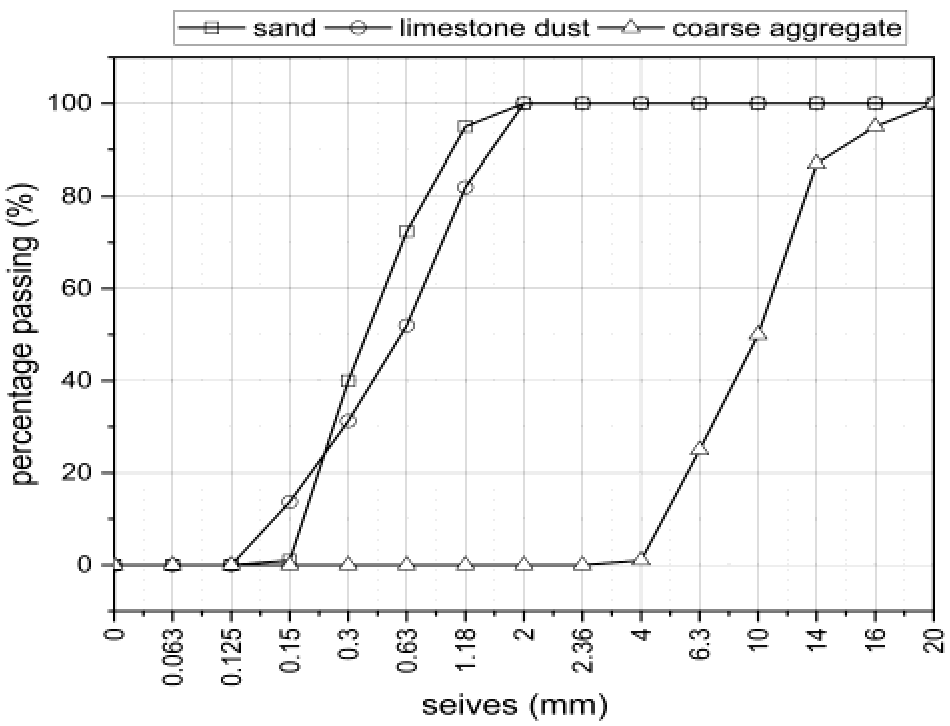

Figure 3. Particle size distribution curves for fine and coarse aggregate

3.2. Method validation

Various HSSCC mixes were designed based on the target compressive strength and rheological properties to validate the proposed methodology. Four series of HSSCC mixes were based on compressive strengths of 70, 80, 90 and 100 MPa, with plastic viscosities ranging from 1.3 to 12 Pa·s. Each series had four mixes with different plastic viscosity values and various sand-to-aggregate (S/A) and paste-to-solid (P/S) ratios. The relative proportions and details of the mixes are given in Tables 4 and 5, respectively. The mixes designated as A and C were designed to contain 48% of sand by the total weight of aggregate (S/A), while B and D were designed for higher S/A ratios. In addition, A and B had lower paste-to-solid ratios than C and D. The maximum cement replacement (indicated in Table 4) was determined as 40% without compromising the target compressive strength based on trial-and-error procedures.

To determine the self-compaction properties, slump flow, J-ring, and L-box tests were conducted in accordance with EFNARC (2005). All tests were video-recorded in the fresh state, and from the recordings, it was noted that none of the mixes showed signs of segregation or bleeding. Fifteen cubes (100 × 100 × 100 mm) were cast from each of the sixteen mixes. After one day, the specimens were de-moulded and cured in water at 20 (±1) °C. The cube compressive strengths were tested at 7, 28 and 90 days according to BS EN 12350-3 (2019).

Table 4. The mix proportions of experimental HSSCC mixes, kg/m^3

Mix code	w/cm	Water	Cementitious material			SP	Aggregates		
							FA		
			Cement	GGBS	Fly ash		Sand	LD	CA
70A	0.40	188.4	282.5	94.2	94.2	2.8	542.6	237.1	839.7
70B		188.4	282.5	94.2	94.2	2.8	593.6	259.4	763.9
70C		197.2	295.8	98.6	98.6	3.0	527.8	230.6	816.8
70D		197.2	295.8	98.6	98.6	3.0	561.4	245.3	766.9
80A	0.35	174.2	298.6	99.5	99.5	3.5	546.0	238.6	845.1
80B		174.2	298.6	99.5	99.5	3.5	604.0	263.9	750.6
80C		181.9	311.8	103.9	103.9	3.6	532.3	232.6	823.8
80D		181. 9	311.8	103.9	103.9	3.6	574.1	250.9	761.7
90A	0.30	164.4	328.8	109.6	109.6	4.4	538.2	235.2	832.9
90B		164.4	328.8	109.6	109.6	4.4	590.0	257.8	756.0
90C		170.2	340.3	113.5	113.5	4.5	527.0	230.3	815.6

90D		170.2	340.3	113.5	113.5	4.5	566.4	247.5	750.0
100A	0.26	151.7	350.0	116.7	116.7	5.8	537.1	234.7	831.3
100B		151.7	350.0	116.7	116.7	5.8	590.6	258.1	751.1
100C		156.0	360.0	120.0	120.0	6.0	528.0	230.7	817.2
100D		156.0	360.0	120.0	120.0	6.0	563.2	246.1	762.8

Note: The mix code number indicates the target compressive strength.

Table 5. Design details of the HSSCC mixes

Mix code	Plastic viscosity (Pa·s)			Sand/total aggregate by weight (%)	Paste/solid by volume
	Paste	Target	Actual		
70A	0.054	1.6	1.60	48.15	0.61
70B		1.8	1.81	52.76	0.61
70C		1.3	1.30	48.15	0.66
70D		1.4	1.39	51.26	0.66
80A	0.075	2.3	2.34	48.14	0.60
80B		2.7	2.68	53.62	0.60
80C		1.9	1.92	48.15	0.64
80D		2	2.10	51.99	0.64
90A	0.18	5	5.00	48.15	0.62
90B		5.5	5.62	52.86	0.62
90C		4.2	4.28	48.15	0.66
90D		4.6	4.59	52.04	0.66
100A	0.39	10	10.68	48.14	0.63
100B		12	12.02	53.05	0.63
100C		9.5	9.40	48.14	0.66
100D		10	10.06	51.48	0.66

4. Results and discussion

4.1. Fresh state

Slump cone tests, J-ring tests, and L-box tests were used to determine the rheological properties of the study HSSCC mixes. Photographic records of the test results for HSSCC mix 70C are shown in Figures 4-6.

The slump flow test was conducted to determine the t_{500} (s) and the flow spread diameter (mm) of the fresh mixes; the results are indicated in Figure 7. Within the flow spread range of 750±100 mm, the spread time varied from 1 to 4.3 s. It was noted that as the plastic viscosity of the mixes increased, the t_{500} increased, despite the increase in the SP content. This correlates with earlier research that reported that the flow time of a mix was determined by the plastic viscosity rather than the content of SP (Abo Dhaheer et al., 2016a).

Figure 4. The final slump flow diameter of mix 70C

Figure 5. J-ring flow test of mix 70C

Figure 6. L-box test of mix 70C

The J-ring test was used to test the ability of the mixes to pass through congested reinforcement bars as a simulation of the passing ability of HSSCC in actual reinforced construction scenarios. A 300 mm diameter J-ring with 12 steel reinforced bars (16 mm diameter, 100 mm height) was selected for this research. Similar to the slump flow test procedure, the J-ring was set in the centre of a horizontal bottom plate and shared the same circle core as the slump cone. The J-ring expansion was taken as the average of the two diameters of the expanded surface perpendicular to the expansion of the slump of the concrete mixture. It can be seen in Figure 8 that the flow time t_{500j} correlated well with the plastic viscosity of the corresponding HSSCC mixes.

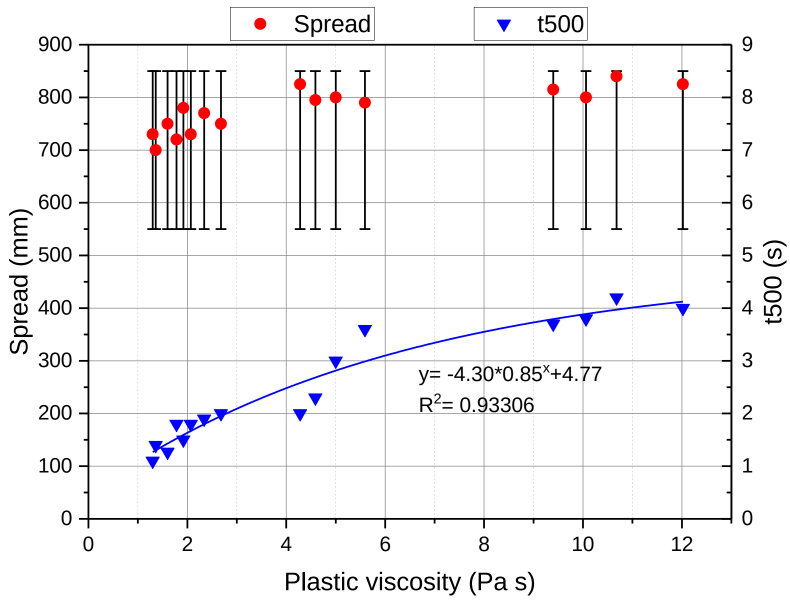

Figure 7. The slump flow diameters and t_{500} relative to plastic viscosity

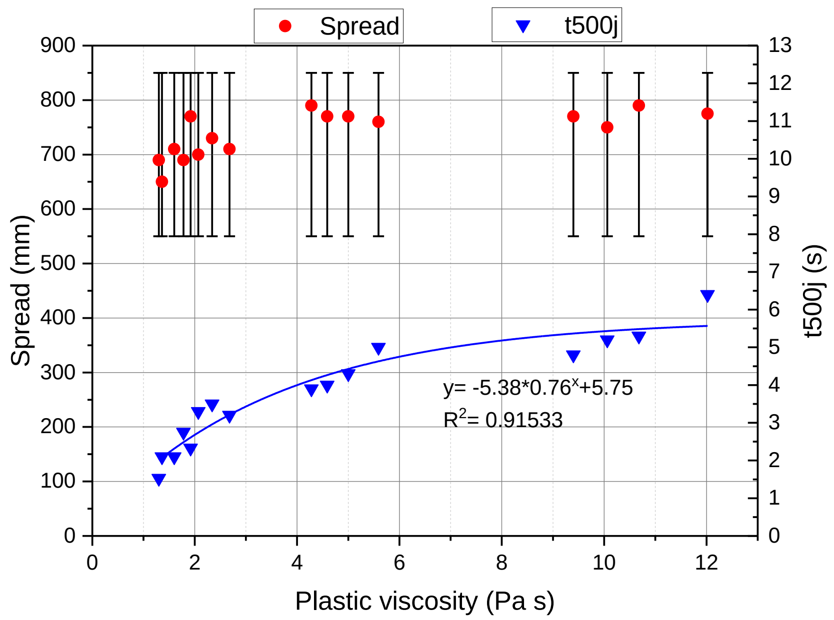

Figure 8. The J-ring flow diameters and t_{500j} relative to plastic viscosity

When comparing the flow time in the slump (t_{500}) and J-ring (t_{500j}) tests, the difference in flow time between these tests increased as the plastic viscosity increased. This can be attributed to specific properties of the viscous fluid, whereby HSSCC mixtures take more time to pass through the reinforced bars as the concrete becomes more viscous. In addition to the flow time, these tests also measured spread diameters; the results are given in Table 6. According to ASTM C1621 (ASTM, 2014), the blocking characteristics can be evaluated by estimating the difference between the flow spread diameters in the slump and J-ring tests. Differences less than 25 mm indicate that there is no visible blocking, differences between 25 and 50 mm indicate minimal to noticeable blocking, while differences greater than 50 mm indicate noticeable to extreme blocking. The results in Table 6 show that the flow spread differences were less than 50 mm, indicating that no extreme blocking occurred during the tests.

Table 6. The flow diameters and differences in slump and J-ring tests

Mix code	D_{slump} (mm)	D_{J-ring} (mm)	$D_{slump} - D_{J-ring}$ (mm)
70A	750	710	40
70B	720	690	30
70C	730	690	40
70D	700	650	50
80A	770	730	40
80B	750	710	40
80C	780	770	10
80D	730	700	30
90A	800	770	30
90B	790	760	30
90C	825	790	35
90D	795	770	25
100A	840	790	50
100B	825	775	50
100C	815	770	45
100D	800	750	50

L-box tests were used to assess the ability of HSSCC mixes to flow through reinforced bars and into a frame under self-weight alone. A two-bar system (12 mm diameter) was selected as comparable to the gap between the bars in the J-ring test. The time was recorded that each HSSCC mix took to reach 200 mm (t_{200}) and 400 mm (t_{400}) in the horizontal direction once the gate was opened. The passing ability (PA) ratio was expressed by the ratio of the depth of concrete at either end of the horizontal leg of the L-box (H1/H2). Figure 9 shows that all mixes passed the Class PA1 in the L-box test according to the European Guidelines for Self-Compacting Concrete (EFNARC, 2005), thus indicating a good filling ability. In addition, the flow time and plastic viscosity showed significant exponential correlation in all HSSCC mixes.

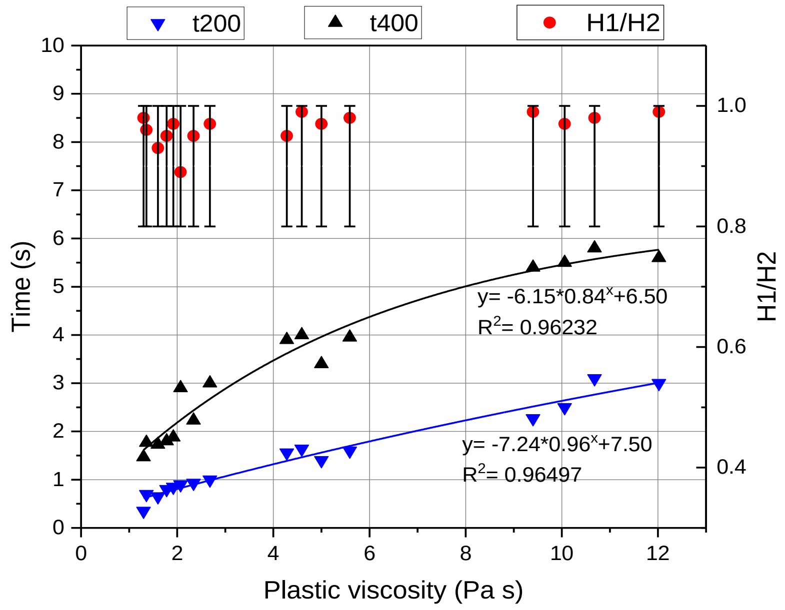

Figure 9. The t_{200} and t_{400} time and passing ability ratios in the L-box test relative to plastic viscosity

The relationship between S/A ratio and slump flow diameter is presented three-dimensionally in Figure 10, which shows that the slump flow diameters decreased as the S/A ratios increased in most of the test samples while the ratios of paste-to-solid and the SP quantity remained constant. This observation is consistent with the results of experimental investigations conducted in previous research (Jovein & Shen, 2016). Although Yardimci et al. (2014) reported an increase in slump flow diameter as the S/A ratio increased from 0.48 to 0.71, this could be attributed to the increased quantity of SP used with the increasing S/A ratios in their mixes.

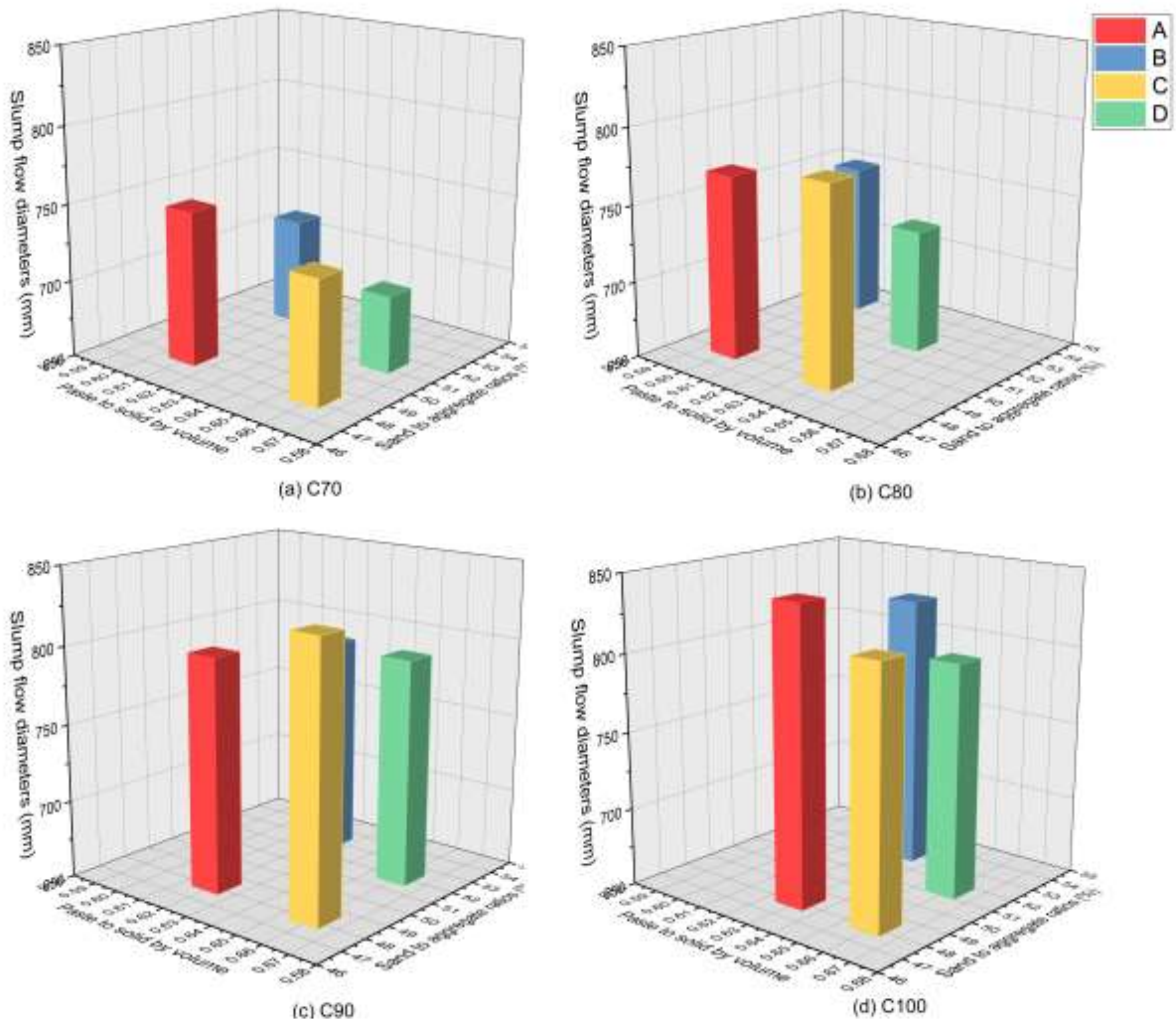

Figure 10. The relationship of sand-to-aggregate ratios and slump flow diameters for mix cases A, B, C and D

4.2. Compressive strength

The results of the compressive strength tests done at 7, 28 and 90 days are presented in Table 7. It has been confirmed that the compressive strength of concrete is predominantly determined by the ratio of water to cementitious materials. Although the mixes with lower sand-to-aggregate (S/A) ratios achieved slightly higher compressive strengths than those with higher S/A ratios, the differences were considered small and insignificant. However, despite the minimal influence of the replacement of natural river sand with the coarser fraction of limestone dust in the fresh and hardened states, such a replacement is economically feasible and environmentally friendly. It can be noted that all mixes achieved close to the target compressive strength at 28 days. Thus, it can be concluded that the proposed mix design method can be efficient and reliable for designing sustainable HSSCC.

Table 7. Compressive strengths of the HSSCC investigated

Target compressive strength (MPa)	Mix code	Compressive strength (MPa)		
		7 days	28 days	90 days
70	70A	48.3	74.9	79.5
	70B	45.3	70.4	75.6
	70C	47.3	70.1	78.8
	70D	48.6	68.6	76.5
80	80A	63.5	80.3	88.3
	80B	62.8	78.4	86.7
	80C	60.6	82.2	92.9
	80D	60.3	81.1	90.1
90	90A	72.3	91.1	101.9
	90B	69.4	88.4	96.4
	90C	71.6	93.2	103.2
	90D	70.4	91.3	98.6
100	100A	80.4	100.2	108.8
	100B	74.5	98.1	106.7
	100C	77.8	100.4	105.4
	100D	76.8	98.3	102.7

4.3. Evaluation of the sustainability performance

The quantity of cement per unit of compressive strength ($(\mathrm{kg/m^3})/\mathrm{MPa}$) used in the four series of this study is presented in Figure 11. It was observed that as the compressive strength increased, the quantity of cement required to attain 1 MPa decreased, with the lowest cement quantity per MPa being achieved with mix 100A ($3.48\ \mathrm{kg/m^3/MPa}$). Moreover, it can be noted from the data presented in Figure 11 that the proposed method required significantly less cement per MPa than the quantity of 5 $(\mathrm{kg/\ m^3})/\mathrm{MPa}$ found in the literature for HSC and HSSCC (Damineli et al., 2010; Deeb et al., 2012; Deeb & Karihaloo, 2013). This validates the effectiveness of the proposed method in reducing cement consumption per MPa of compressive strength.

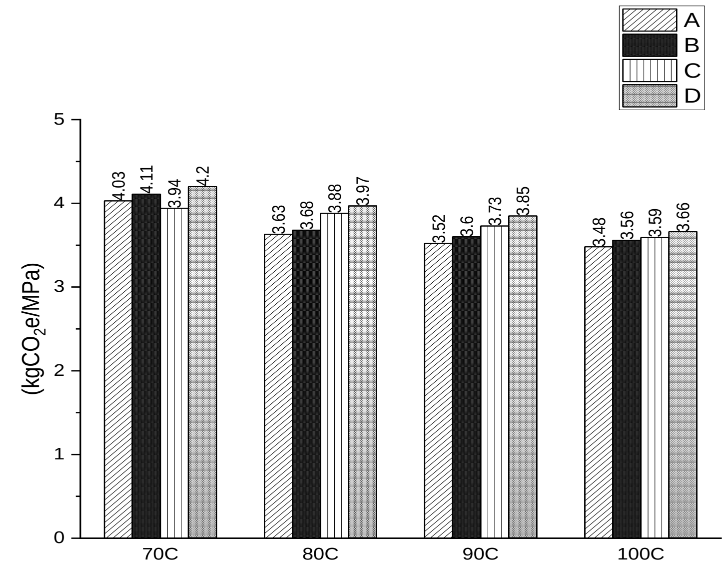

Figure 11. Quantity of cement required to achieve 1 MPa of compressive strength at 28 days for the proposed mixes

Sustainability investigations were conducted to determine the carbon dioxide emissions for each material (Table 8) according to the literature. The carbon dioxide emissions and cement consumption required to achieve 1 MPa of compressive strength were subsequently factored into the efficiency calculations.

Table 8. CO_2 emission factors of fine materials, aggregates and SP collected from the literature

Materials	CO_2 emissions (kgCO_2/kg)	Reference
Cement	0.931	(Hanif et al., 2017)
GGBS	0.0796	(Mineral Products Association, 2015)
Fly ash	0.0001	(Mineral Products Association, 2015)
Natural river aggregates	0.003	(Hanif et al., 2017)
Natural coarse aggregate	0.007	(Hanif et al., 2017)
Limestone (stone powder)	0.0016	(Campos et al., 2020)
SP	0.250	(Hanif et al., 2017)

Figure 12 shows the calculated quantities of CO_2 emissions per cubic metre of the proposed mixes (kgCO_2e/m^3). It can be observed that CO_2 emissions per cubic metre increased as the strength increased, which can be ascribed to the increased cement quantities associated with the increased strengths. One proposed method to reduce the CO_2 emissions of concrete is by using industrial by-products with lower CO_2 emission values. In the current study, this was done by replacing 40% of the cement with pozzolanic materials (GGBS and fly ash) by weight and 30% of the sand with limestone dust by volume. It was noted that the change in carbon dioxide emissions was mainly due to the cement replacement, which correlated with the results indicated in the literature (Celik et al., 2015). However, the sand replacement in the mixes had negligible effects on the emissions. For example, partially replacing the cement in mix 100A reduced CO_2 emissions by 37.80%, while partially replacing the sand reduced the emissions by 0.72%. Nevertheless, as mentioned previously, replacing natural river sand with a coarser fraction of limestone dust is economically feasible and environmentally friendly and increases the durability of the concrete (Kirthika et al., 2020).

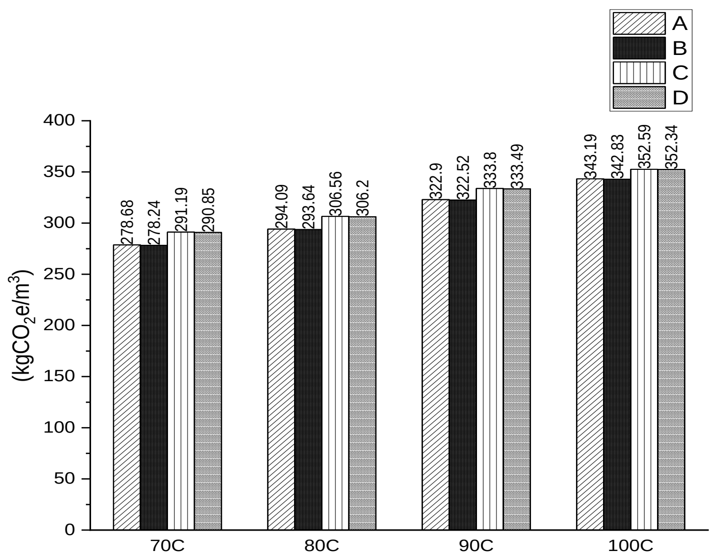

Figure 12. The carbon dioxide per cubic metre of the produced mixes in the present study

A further approach to reducing the cement consumption and CO_2 emissions of concrete is to use less concrete. This can be achieved by increasing the compressive strength of the concrete and hence lowering the quantity of concrete required to carry the same load. The efficiency in this regard can be assessed by considering the amount of carbon dioxide emitted to achieve 1 MPa of the concrete compressive strength (Campos et al., 2020). Figure 13 presents the CO_2 emissions of the studied mixes to attain 1MPa of compressive strength (kgCO_2 e/MPa) at 28 days. Mix 100A showed the lowest carbon dioxide emissions per MPa (3.4 kgCO_2 e/MPa) to obtain 1 MPa of compressive strength at 28 days. When the quantity of cement used for each mix was compared to its respective CO_2 emissions to obtain 1 MPa, it was noted that these were proportional (Figures 11 and 13).

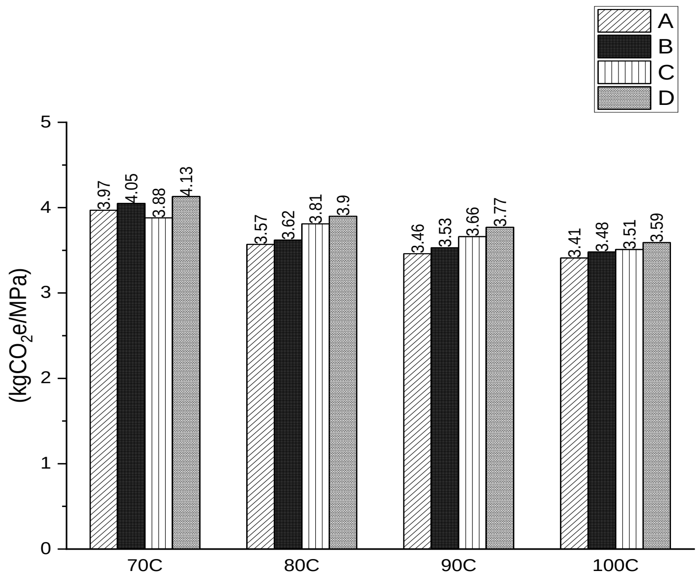

Figure 13. The carbon dioxide emissions of the proposed mixes required to achieve 1 MPa of compressive strength at 28 days

The analysis by Rahla et al. (2019) demonstrated that using GGBS or fly ash resulted in concrete with lower environmental impacts and cost, thus achieving greater sustainability. Wang et al. (2017) conducted a sustainability assessment to integrate the environmental, economic, and social performance of such concrete into a single value. It was found that increasing the fly ash content of concrete improved the sustainability performance in all three areas. Further research could be conducted using other waste materials, such as rice husk ash, in mix designs to provide guidance toward greener high-strength self-compacting concrete (HSSCC).

These fundamental results, together with the analysis of the current study, show that HSSCC can improve the properties of concrete and its sustainability. Therefore, the proposed mix design in this study can be effectively used to optimise the HSSCC performance and decrease the consumption of dwindling non-renewable resources with their associated CO_2 emissions. Increasing the compressive strength of the concrete can lead to lower cement consumption, lower CO_2 emissions, and reduced costs. Hence, economic and environmental aspects can be improved by using the proposed design methodology for HSSCC mixtures.

5. Conclusions

This paper developed an effective mix-proportioning procedure for designing sustainable HSSCC, using GGBS and fly ash as cement replacement materials, based on target compressive strength and plastic viscosity. The target plastic viscosity of the HSSCC mixes was based on the rheology of the paste and micro-mechanical constitutive models. This method also predicted the compressive strengths of the concrete mixes with target values of 70 MPa, 80 MPa, 90 MPa, and 100 MPa, by controlling the water-to-cementitious material ratio. Design charts were derived in this study to enable the straightforward application of the proposed methodology. The sustainability performance of HSSCC can be enhanced by several approaches, such as the reduction of cement and non-renewable materials. Pozzolanic materials (GGBS and fly ash) and limestone dust partially replaced cement and natural river sand without compromising the concrete's fresh and hardened mechanical properties. A further approach for enhancing the sustainability performance of HSSCC can be achieved by using less concrete with greater compressive strength. The rates of CO_2 emissions and cement consumption to produce one unit of compressive strength (MPa) were significantly lower for the study mixes than those found in the literature. The proposed method was successfully validated through an extensive experimental investigation, and all mixtures achieved the designed targets and satisfied the requirement of self-compacting concrete criteria. It can be concluded that the proposed mix-proportioning method is highly effective in producing HSSCC with the required fresh and hardened properties while being environmentally friendly.

Disclosure statement

The authors report that there are no competing interests to declare.

ORCID

Abdullah Alshahrani https://orcid.org/0000-0002-2454-3427
Tianyi Cui https://orcid.org/0000-0002-6252-6302
Ayman Almutlaqah https://orcid.org/ 0000-0002-7744-1686
Sivakumar Kulasegaram https://orcid.org/0000-0002-9841-1339

References

Abo Dhaheer, M. S., Al-Rubaye, M. M., Alyhya, W. S., Karihaloo, B. L., & Kulasegaram, S. (2016a). Proportioning of self–compacting concrete mixes based on target plastic viscosity and compressive strength: Part I - mix design procedure. *Journal of Sustainable Cement-Based Materials*, *5*(4), 199–216. https://doi.org/10.1080/21650373.2015.1039625

Abo Dhaheer, M. S., Al-Rubaye, M. M., Alyhya, W. S., Karihaloo, B. L., & Kulasegaram, S. (2016b). Proportioning of self-compacting concrete mixes based on target plastic viscosity and compressive strength: Part II - experimental validation. *Journal of Sustainable Cement-Based Materials*, *5*(4), 217–232. https://doi.org/10.1080/21650373.2015.1036952

Adesina, A., & Awoyera, P. (2019). Overview of trends in the application of waste materials in self-compacting concrete production. *SN Applied Sciences*, *1*(9), 1–18. https://doi.org/10.1007/s42452-019-1012-4

Aggarwal, P., & Aggarwal, Y. (2019). Strength properties of SCC. In R. Siddique (Ed.), *Self-Compacting Concrete: Materials, Properties and Applications* (pp. 83–115). Woodhead Publishing. https://doi.org/10.1016/B978-0-12-817369-5.00004-0

Aïtcin, P. C. (2019). The influence of the water/cement ratio on the sustainability of concrete. *Lea's Chemistry of Cement and Concrete*, 807–826. https://doi.org/10.1016/B978-0-08-100773-0.00017-4

Al-Oran, A. A. A., Safiee, N. A., & Nasir, N. A. M. (2019). Fresh and hardened properties of self-compacting concrete using metakaolin and GGBS as cement replacement. *European Journal of Environmental and Civil Engineering*, 1–14. https://doi.org/10.1080/19648189.2019.1663268

ASTM C1621. (2014). *Standard Test Method for Passing Ability of Self-Consolidating Concrete by J-Ring*. American Society for Testing and Materials.

Berndt, M. L. (2015). Influence of concrete mix design on CO2 emissions for large wind turbine foundations. *Renewable Energy*, *83*, 608–614. https://doi.org/10.1016/j.renene.2015.05.002

BS EN 12350-11. (2010). *BSI Standards Publication Testing fresh concrete Part 18.*

Campos, H. F., Klein, N. S., & Marques Filho, J. (2020). Proposed mix design method for sustainable high-strength concrete using particle packing optimization. *Journal of Cleaner Production*, *265*, 121907. https://doi.org/10.1016/j.jclepro.2020.121907

Campos, H. F., Richa, T. M. S., Reus, G. C., Klein, N. S., & Marques filho, J. (2019). Determination of the optimal replacement content of Portland cement by stone powder using particle packing methods and analysis of the influence of the excess water on the consistency of pastes. *Revista IBRACON de Estruturas e Materiais*, *12*(2), 210–232. https://doi.org/10.1590/s1983-41952019000200002

Celik, K., Meral, C., Petek Gursel, A., Mehta, P. K., Horvath, A., & Monteiro, P. J. M. (2015). Mechanical properties, durability, and life-cycle assessment of self-consolidating concrete mixtures made with blended portland cements containing fly ash and limestone powder. *Cement and Concrete Composites*, *56*, 59–72. https://doi.org/10.1016/j.cemconcomp.2014.11.003

Damineli, B. L., Kemeid, F. M., Aguiar, P. S., & John, V. M. (2010). Measuring the eco-efficiency of cement use. *Cement and Concrete Composites*, *32*(8), 555–562. https://doi.org/10.1016/j.cemconcomp.2010.07.009

de Grazia, M. T., Sanchez, L. F. M., Romano, R. C. O., & Pileggi, R. G. (2019). Investigation of the use of continuous particle packing models (PPMs) on the fresh and hardened properties of low-cement concrete (LCC) systems. *Construction and Building Materials*, *195*, 524–536. https://doi.org/10.1016/j.conbuildmat.2018.11.051

de Kruif, C. G., van Iersel, E. M. F., Vrij, A., & Russel, W. B. (1985). Hard sphere colloidal dispersions: Viscosity as a function of shear rate and volume fraction. *The Journal of Chemical Physics*, *83*(9), 4717–4725. https://doi.org/10.1063/1.448997

de la Rosa, Á., Poveda, E., Ruiz, G., & Cifuentes, H. (2018). Proportioning of self-compacting steel-fiber reinforced concrete mixes based on target plastic viscosity and compressive strength: Mix-design procedure & experimental validation. *Construction and Building Materials*, *189*, 409–419. https://doi.org/10.1016/j.conbuildmat.2018.09.006

de Matos, P. R., Sakata, R. D., & Prudêncio, L. R. (2019). Eco-efficient low binder high-performance self-compacting concretes. *Construction and Building Materials*, *225*, 941–955. https://doi.org/10.1016/j.conbuildmat.2019.07.254

Deeb, R., Ghanbari, A., & Karihaloo, B. L. (2012). Development of self-compacting high and ultra high performance concretes with and without steel fibres. *Cement and Concrete Composites*, *34*(2), 185–190. https://doi.org/10.1016/j.cemconcomp.2011.11.001

Deeb, R., & Karihaloo, B. L. (2013). Mix proportioning of self-compacting normal and high-strength concretes. *Magazine of Concrete Research*, *65*(9), 546–556. https://doi.org/10.1680/macr.12.00164

Domone, P. L. (2006). Self-compacting concrete: An analysis of 11 years of case studies. *Cement and Concrete Composites*, *28*(2), 197–208. https://doi.org/10.1016/j.cemconcomp.2005.10.003

EFNARC. (2005). *The European Guidelines for Self-Compacting Concrete*. www.efnarc.org

Feys, D., Heirman, G., de Schutter, G., Verhoeven, R., Vandewalle, L., & van Gemert, D. (2007). Comparison of two concrete rheometers for shear thickening behaviour of SCC. *5th Int. RILEM Symposium on Self-Compacting Concrete*, *1*, 1–6.

Feys, D., & Khayat, K. H. (2013). Comparing Rheological Properties of SCC Obtained with the ConTec and ICAR Rheometers. *Fifth North American Conference on the Design and Use of Self-Consolidating Concrete, 12-15 May, July 2017*, 1–11.

Ghanbari, A., & Karihaloo, B. L. (2009). Prediction of the plastic viscosity of self-compacting steel fibre reinforced concrete. *Cement and Concrete Research*, *39*(12), 1209–1216. https://doi.org/10.1016/j.cemconres.2009.08.018

Gupta, N., Siddique, R., & Belarbi, R. (2021). Sustainable and Greener Self-Compacting Concrete incorporating Industrial By-Products: A Review. *Journal of Cleaner Production*, *284*. https://doi.org/10.1016/j.jclepro.2020.124803

Hanif, A., Kim, Y., Lu, Z., & Park, C. (2017). Early-age behavior of recycled aggregate concrete under steam curing regime. *Journal of Cleaner Production*, *152*, 103–114. https://doi.org/10.1016/j.jclepro.2017.03.107

Jalal, M., Pouladkhan, A., Harandi, O. F., & Jafari, D. (2015). Comparative study on effects of Class F fly ash, nano silica and silica fume on properties of high performance self compacting concrete. *Construction and Building Materials*, *94*, 90–104. https://doi.org/10.1016/j.conbuildmat.2015.07.001

Jawahar, J. G., Sashidhar, C., Reddy, I. V. R., & Peter, J. A. (2013). Effect of coarse aggregate blending on short-term mechanical properties of self compacting concrete. *Materials and Design*, *43*, 185–194. https://doi.org/10.1016/j.matdes.2012.06.063

Jovein, H. B., & Shen, L. (2016). Effects of aggregate properties on rheology of self-consolidating concrete. *Advances in Civil Engineering Materials*, *5*(1), 235–255. https://doi.org/10.1520/ACEM20160008

Kaish, A. B. M. A., Breesem, K. M., & Abood, M. M. (2018). Influence of pre-treated alum sludge on properties of high-strength self-compacting concrete. *Journal of Cleaner Production*, *202*, 1085–1096. https://doi.org/10.1016/j.jclepro.2018.08.156

Karihaloo, B. L., & Ghanbari, A. (2012). Mix proportioning of selfcompacting high-and ultrahigh-performance concretes with and without steel fibres. *Magazine of Concrete Research*, *64*(12), 1089–1100. https://doi.org/10.1680/macr.11.00190

Kirthika, S. K., Singh, S. K., & Chourasia, A. (2020). Alternative fine aggregates in production of sustainable concrete- A review. *Journal of Cleaner Production*, *268*. https://doi.org/10.1016/j.jclepro.2020.122089

Koehler, E. P., & Fowler, D. W. (2007). *Aggregates in Self-Consolidating Concrete* Aggregates Foundation for Technology. *Research and Education, Research Report ICAR*.

Krieger, I. M., & Dougherty, T. J. (1959). A Mechanism for Non-Newtonian Flow in Suspensions of Rigid Spheres. *Transactions of the Society of Rheology*, *3*(1), 137–152. https://doi.org/10.1122/1.548848

Long, G., Gao, Y., & Xie, Y. (2015). Designing more sustainable and greener self-compacting concrete. *Construction and Building Materials*, *84*, 301–306. https://doi.org/10.1016/j.conbuildmat.2015.02.072

Mineral Products Association. (2015). *Fact Sheet 18: Embodied CO 2 e of UK cement , additions and cementitious material*. https://cement.mineralproducts.org/documents/Factsheet_18.pdf

Nehdi, M., Pardhan, M., & Koshowski, S. (2004). Durability of self-consolidating concrete incorporating high-volume replacement composite cements. *Cement and Concrete Research*, *34*(11), 2103–2112. https://doi.org/10.1016/j.cemconres.2004.03.018

Okamura, H., & Ouchi, M. (1999). Self-compacting concrete, present use and future. In *1st International RILEM Symposium on Self-Compacting Concrete* (pp. 3–14).

Rahla, K. M., Mateus, R., & Bragança, L. (2019). Comparative sustainability assessment of binary blended concretes using Supplementary Cementitious Materials (SCMs) and Ordinary Portland Cement (OPC). *Journal of Cleaner Production*, *220*, 445–459. https://doi.org/10.1016/j.jclepro.2019.02.010

Shi, C., Wu, Z., Lv, K., & Wu, L. (2015). A review on mixture design methods for self-compacting concrete. *Construction and Building Materials*, *84*, 387–398. https://doi.org/10.1016/j.conbuildmat.2015.03.079

Sivakrishna, A., Adesina, A., Awoyera, P. O., & Kumar, K. R. (2020). Green concrete: A review of recent developments. *Materials Today: Proceedings*, *27*, 54–58. https://doi.org/10.1016/j.matpr.2019.08.202

Struble, L., & Sun, G. K. (1995). Viscosity of Portland cement paste as a function of concentration. *Advanced Cement Based Materials*, *2*(2), 62–69. https://doi.org/10.1016/1065-7355(95)90026-8

Thomas, B. S., Yang, J., Bahurudeen, A., Abdalla, J. A., Hawileh, R. A., Hamada, H. M., Nazar, S., Jittin, V., & Ashish, D. K. (2021). Sugarcane bagasse ash as supplementary cementitious material in concrete – a review. *Materials Today Sustainability*, *15*. https://doi.org/10.1016/j.mtsust.2021.100086

Wallevik, O. H., & Wallevik, J. E. (2011). Rheology as a tool in concrete science: The use of rheographs and workability boxes. *Cement and Concrete Research*, *41*(12), 1279–1288. https://doi.org/10.1016/j.cemconres.2011.01.009

Wang, J. J., Wang, Y. F., Sun, Y. W., Tingley, D. D., & Zhang, Y. R. (2017). Life cycle sustainability assessment of fly ash concrete structures. *Renewable and Sustainable Energy Reviews*, *80* (1162–1174. https://doi.org/10.1016/j.rser.2017.05.232

Yardimci, M. Y., Baradan, B., & Taşdemir, M. A. (2014). Effect of fine to coarse aggregate ratio on the rheology and fracture energy of steel fibre reinforced self-compacting concretes. *234Sadhana - Academy Proceedings in Engineering Sciences*, *39*(6), 1447–1469. https://doi.org/10.1007/s12046-014-0257-2

Yousuf, S., Sanchez, L. F. M., & Shammeh, S. A. (2019). The use of particle packing models (PPMs) to design structural low cement concrete as an alternative for construction industry. *Journal of Building Engineering*, *25*. https://doi.org/10.1016/j.jobe.2019.100815

Appendix

Example of mix proportioning of high strength SCC

Following the procedural steps in Figure 2, the target compressive strength and plastic viscosity are selected, and the w/cm ratio is calculated. From this, the quantities of cementitious materials and fine aggregate can be determined, and the coarse aggregate quantity can be determined. An example of the mix proportioning procedure is given below for a mix with a target compressive strength of 70 MPa and plastic viscosity of 3 Pa·s. The applicable design chart is given in Figure 14.

- For 70 MPa target compressive strength, the (w/cm) ratio can be calculated by using Equation 1:

  $$f_{cu} = \frac{195}{12.65^{w/cm}}$$

  As f_{cu} = 70 MPa, then $w/cm = 0.40$

- Quantify the cementitious materials (cm) for plastic viscosity $\eta_{mix} = 3\ Pa \cdot s$:

  From Figure 14, $cm/\ \eta\ =\ 140.237\ kg/Pa\ s$ (indicated by the grey curve)

  For $\eta = 3Pa \cdot s$, $cm =\ 420.71\ kg/m^3$.

  The cement is replaced by 20% each of GGBS and fly ash; therefore,

  $Cement\ = 252.43\ kg/m^3$, $GGBS\ = 84.14\ kg/m^3$ and $fly\ ash\ = 84.14\ kg/m^3$

- Calculate the water content.

  As $w/cm = 0.40$, then $w = 0.4 * 420.71 = 168.28$ kg/m^3.

- Assume SP content according to the manufacturer's recommendation.

  As a trial SP dosage, m_{sp}/m_{cm} was assumed to be 0.7%.

  As $cm = 420.71\ kg/m^3$, then SP = 2.95 kg/m^3.

- Calculate the solid phase component contents, fine aggregates (FA) coarse aggregates (CA).

  From Figure 14, $(cm + FA)/\eta = 425.72\ kg/m^3$ (indicated by the red curve)

  As $\eta_{mix} = 3\ Pa\ s$ and $cm = 420.71\ kg/m^3$,

  then $FA = 856.45\ kg/m^3$

  From Figure 14, $(cm + FA + CA)/\eta =\ 711.21\ kg/m^3$ (indicated by the blue curve)

  As $\eta = 3\ Pa$; $cm = 420.71\ kg/m^3$; $FA = 856.45\ kg/m^3$, then $CA = 856.47\ kg/m^3$

- Check if the total volume (T_V) of the concrete mix = 1 m^3.

  The densities of cement, fly ash, GGBS, water, superplasticiser, natural river sand, and coarse aggregate are 3150, 2400, 2400, 1000, 1070, 2550 and 2650, respectively.

$$T_V = \frac{252.43}{3150} + \frac{84.14}{2400} + \frac{84.14}{2400} + \frac{168.28}{1000} + \frac{2.95}{1070} + \frac{856.45}{2550} + \frac{856.47}{2650} + 0.02 = 1m^3$$

- Determine the plastic viscosity of the mix (η_{mix}) by using Equation 6.

$$\phi_{FA} = \frac{\frac{FA}{\rho_{FA}}}{\frac{c}{\rho_c} + \frac{GGBS}{\rho_{GGBS}} + \frac{fly\ ash}{\rho_{fly\ ash}} + \frac{w}{\rho_w} + \frac{SP}{\rho_{SP}} + \frac{FA}{\rho_{FA}} + 0.02} = 0.4960$$

$$\phi_{CA} = \frac{\frac{CA}{\rho_{CA}}}{\frac{c}{\rho_c} + \frac{GGBS}{\rho_{GGBS}} + \frac{fly\ ash}{\rho_{fly\ ash}} + \frac{w}{\rho_w} + \frac{SP}{\rho_{SP}} + \frac{FA}{\rho_{FA}} + \frac{CA}{\rho_{CA}} + 0.02} = 0.3231$$

$$\eta_{mix} = \eta_{paste} * \left(1 - \frac{\phi_{\ fine\ agg}}{\phi_{\ m}}\right)^{-1.9} * \left(1 - \frac{\phi_{coarse\ agg}}{\phi_{\ m}}\right)^{-1.9}$$

$$= 0.054 * \left(1 - \frac{0.4960}{0.63}\right)^{-1.9} * \left(1 - \frac{0.3231}{0.74}\right)^{-1.9} = 3.042\ Pa\ s$$

where η_{paste} obtained by viscometer $= 0.054$

- The difference between the desired viscosity and the calculated viscosity is therefore:

  $D = (3.056 - 3)/3 = 1.4\% < 5\%$, which is in the acceptable range.

- The final mix proportions are shown in Table 8.

Table 8. Mix ingredients of C70 HSSCC mix with plastic viscosity of 3 Pa s

Materials	water	cement	GGBS	Fly ash	SP	FA	CA
Mass (kg/m^3)	168.28	252.43	84.14	84.14	2.95	856.45	856.47

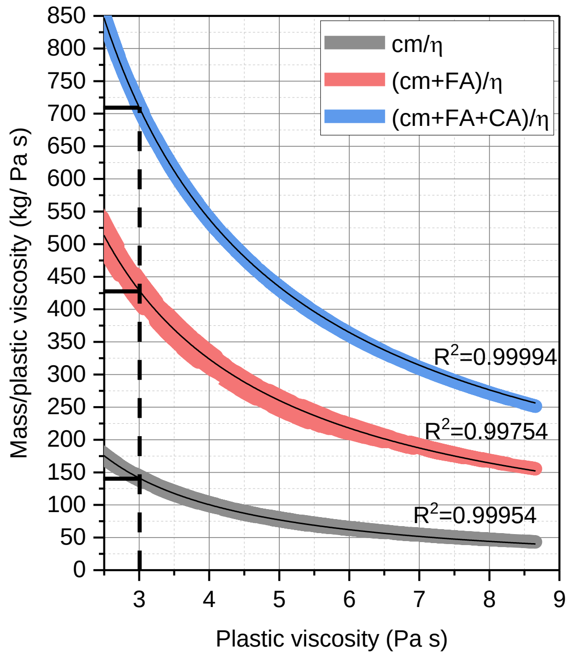

Figure 14. Design chart for 70 MPa HSSCC